Towards 4-D Cardiac Reconstruction without ECG and Motion Periodicity using C-arm CT

Christopher Rohkohl, Günter Lauritsch, Marcus Prümmer, Jan Boese and Joachim Hornegger

***Abstract*—Heart motion is a crucial problem in cardiac tomographic cone-beam image reconstruction. It requires special treatment to avoid motion related image artifacts. Analytic and iterative algorithms for approximative and exact motion compensated 3-D reconstruction are known. The estimation of the motion field from the projection data is still an open problem. The inherent assumption of recent publications is a periodic heart motion. The electrocardiogram (ECG) is used as an estimate for the periodically repeating heart phase. In those approaches the heart motion is averaged over several heart cycles. As a consequence heart beat variabilities cannot be captured. However, frequently arrhytmic heart cycles can be observed in a clinical environment. In addition breathing motion can still occur.**

We present a reconstruction method based on a 4-D time-continuous B-spline motion field which is parameterized by the acquisition time and not the quasi-periodic heart phase. A time-correlated objective function is introduced which measures the error between the measured projection data and the dynamic forward projection of the motion compensated reconstruction. For reconstruction an analytic motion compensation algorithm is used. Our objective function formulation exploits the fact that the desired motion compensated reconstruction is totally determined by a given motion field. The motion model parameters are estimated using an iterative optimization scheme. Simulation results are provided for a synthetic cardiac vasculature phantom undergoing deformable motion which could be well recovered using the presented framework without using the ECG and assuming periodicity of the motion.

***Index Terms*—Motion estimation, motion compensation, 4-D reconstruction**

I. Introduction

THE tomographic 3-D cone-beam reconstruction of moving objects is of high importance for many applications, e.g. in the medical field. Patient or organ motion degrades the image quality of 3-D reconstructions and thus is in the focus of many current research activities especially in cardiac applications. With the technology of C-arm CT it is possible to reconstruct intraprocedural 3-D images from angiographic projection data [1]. However, cardiac reconstruction is yet a challenging problem due to the long acquisition time of several seconds at which several heart beats occur, leading to motion related image artifacts, e.g. blurring or streaks.

An established technique for time-resolved cardiac reconstruction is to record the electrocardiogram (ECG) during the data acquisition. Based on the ECG-signal a relative cardiac phase is assigned to each projection image assuming a cyclic heart motion [2]. The phase information is used for a phase-correlated reconstruction by gating or motion estimation and compensation. A gated reconstruction takes only those images into account that lie inside a defined temporal window, that is centered at the targeting reconstruction phase [3], [4], [5]. This is however not ideal in terms of missing data and residual motion. To increase the data usage motion compensated reconstruction algorithms [6], [7], [8], [4] are applied. The phase information is used during motion estimation to parameterize a motion field that maps every heart phase to the target phase by some kind of registration operation [6], [9], [10]. Another approach is the integration of the motion estimation directly into iterative reconstruction algorithms. The periodic motion model parameters and the reconstruction are jointly estimated during the optimization [11], [12].

The common problem of the previous approaches is that the averaged periodic motion model does not necessarily represent accurately the actual heart motion of each individual beat. Thus the quality of the motion correction and periodicity assumption are correlated. Accordingly, the previous methods were shown to provide reasonable results in the presence of regular heart rates without breathing or other patient motion. However, patients requiring 3-D imaging of the heart are likely to suffer from heart diseases and cannot completely hold breath, stay still or have irregular heart beats. Those aspects do conflict with the periodicity assumption. Up to now, these problems were addressed by approximate 2-D corrections in the projection image. Blondel et al. [6] proposed to model breathing motion of the heart as a translation mainly in axial direction. Hansis et al. [13] proposed to cope with the problem by performing a 2-D/2-D registration of the projection image with a forward projection of an initial reconstruction. However, none of the methods can cope with the general case of non-cyclic 3-D motion.

In this paper a method for the cardiac 4-D reconstruction without perodicity assumption is introduced. We propose to separate the estimation of the motion field from the image reconstruction using an analytic motion compensation algorithm. It is exploited that given a motion compensated reconstruction algorithm, the desired image volume is totally determined by the motion field. This representation allows motion estimation for non-periodic deformable motions using an iterative optimization scheme. The motion parameters are estimated such that the error between the measured projection data and the dynamic forward projection of the corresponding motion compensated reconstruction is minimized.

C. Rohkohl, M. Prümmer and J. Hornegger are with the Chair of Pattern Recognition, Department of Computer Science, Friedrich-Alexander University Erlangen-Nuremberg, Martensstr. 3, 91058 Erlangen, Germany.

G. Lauritsch and J. Boese are with the Siemens AG, Healthcare Sector, Siemensstr. 1, 91301 Forchheim, Germany.

Corresponding author: C. Rohkohl (christopher.rohkohl@informatik.uni-erlangen.de)

II. METHODS

This part of the paper is organized as follows. In Sect. II-A an overview of formalisms and notation is provided. Next, in Sect. II-B the objective function for motion estimation is introduced. The upcoming Sections II-C and II-D contain the explicit formulation of the non-periodic 4-D B-spline motion model and motion compensated reconstruction, respectively. Finally, in Sect. II-E the optimization strategy is discussed.

A. Preliminaries

Some basic assumptions about the data and motion model:

- Projection data mapping $p : \{1, \dots, N\} \times \mathbb{R}^2 \to \mathbb{R}$: The projection data mapping $p(i, \boldsymbol{u})$ returns the measured image value of the i-th projection image at the pixel $\boldsymbol{u}$. The number of projection images is denoted N.
- Projection function $A : \{1, \dots, N\} \times \mathbb{R}^3 \to \mathbb{R}^2$: The projection function $A(i, \boldsymbol{x}) = \boldsymbol{u}$ maps a voxel $\boldsymbol{x}$ to a pixel location $\boldsymbol{u}$ in the i-th projection image.
- Set of voxels $L_{i,\boldsymbol{u}} = \{\, \boldsymbol{x} \in \mathbb{R}^3 \mid A(i, \boldsymbol{x}) = \boldsymbol{u} \,\}$: The voxels $\boldsymbol{x} \in L_{i,\boldsymbol{u}}$ form a straight ray hitting the detector bin $\boldsymbol{u}$ at projection number i.
- Motion model $M : \{1, \dots, N\} \times \mathbb{R}^3 \times \mathbb{S} \to \mathbb{R}^3$: The motion model is an invertable function $M(i, \boldsymbol{x}, \boldsymbol{s}) = \boldsymbol{x}'$ mapping a voxel coordinate $\boldsymbol{x}$ for the i-th projection image to a new location $\boldsymbol{x}'$. It depends on the motion model paramters $\boldsymbol{s} \in \mathbb{S}$. The concrete 4-D B-spline motion model used in this paper and the corresponding parameter space $\mathbb{S}$ are detailed in Sect. II-C.
- Motion compensated reconstruction $f : \mathbb{R}^3 \times \mathbb{S} \to \mathbb{R}$: The function $f(\boldsymbol{x}, \boldsymbol{s})$ returns the reconstructed object value at the voxel coordinate $\boldsymbol{x}$ based on the motion model parameters $\boldsymbol{s} \in \mathbb{S}$. It depends not only on the voxel location as in the static case, but also on the motion model parameters which define the object motion. The concrete reconstruction algorithm used in this paper is detailed in Sect. II-D.

B. Objective Function for Motion Estimation

Motion estimation is formulated as a multi-dimensional optimization problem where the motion model parameters $\hat{\boldsymbol{s}} \in \mathbb{S}$ minimizing the objective function $\mathcal{L} : \mathbb{S} \to \mathbb{R}$ need to be estimated, i.e.

$$\hat{\boldsymbol{s}} = \arg\min_{\boldsymbol{s} \in \mathbb{S}} \mathcal{L}(\boldsymbol{s}) \,. \tag{1}$$

The objective function introduced in this paper is motivated by the basic relationship of the motion compensated reconstruction f with the measured projection data p. Digital Reconstructed Radiographs (DRRs) can be created from a reconstruction $f(\boldsymbol{x}, \boldsymbol{s})$ by dynamic forward projection:

$$r(i, \boldsymbol{u}, \boldsymbol{s}) = \sum_{\boldsymbol{x} \in L_{i,\boldsymbol{u}}} f\left(M^{-1}(i, \boldsymbol{x}, \boldsymbol{s}), \boldsymbol{s}\right) . \tag{2}$$

The function $r : \{1, \dots, N\} \times \mathbb{R}^2 \times \mathbb{S} \to \mathbb{R}$ returns the dynamic forward projection of the motion compensated reconstruction f. The voxels on the straight ray $L_{i,\boldsymbol{u}}$ are transformed by the inverse motion model to consider the motion state observed at the projection image i.

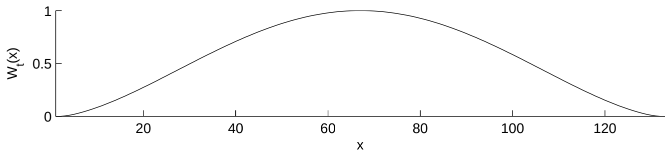

Fig. 1: Temporal weighting function $W_t(x)$ for the parameters $e_t = 1.5, c_t = 67, w_t = 130$.

The matching of the measured data p and forward projected data r is assessed using a pixel-wise dissimilarity measure $d : \mathbb{R} \times \mathbb{R} \to \mathbb{R}$, e.g. the squared error $d(x, y) = (x - y)^2$. Formally, our objective function is then given by:

$$\mathcal{L}(\boldsymbol{s}) = \sum_i W_t(i) \left(\sum_{\boldsymbol{u}} d\left(p(i, \boldsymbol{u}), r(i, \boldsymbol{u}, \boldsymbol{s})\right) \right) . \tag{3}$$

The term $W_t : \mathbb{R} \to [0, 1]$ is a temporal weighting function which is introduced to obtain time-correlated motion model parameters. It is required because without the additional weighting term several solutions to the optimization problem exist. Each set of motion model parameters at a certain point in time that encodes the relative motion to all other points in time is a minimizer of (1). This is problematic as it might lead to an alternation between different solutions during the optimization and can prevent convergence. The temporal weighting function is given by

$$W_t(x) = \begin{cases} \cos^{e_t}\left(\frac{|c_t - x|}{w_t}\pi\right) & \text{if } |c_t - x| \le \frac{w_t}{2} \\ 0 & \text{otherwise.} \end{cases} \tag{4}$$

In Fig. 1 an example of the temporal weighting function is depicted for $e_t = 1.5, c_t = 67, w_t = 130$.

C. Non-periodic 4-D B-Spline Motion Model

We assume a time-continous motion model that maps a voxel $\boldsymbol{x} = (x_0, x_1, x_2)^T$ to a new voxel location $\boldsymbol{x}'$ for each projection image. The mapping is based on the motion model paramters $\boldsymbol{s} \in \mathbb{S}$. In this work, a 4-D B-spline is used. It has been shown to be suitable to describe cardiac motion numerous times [6], [10], [12] as it guarantees a locally and temporally smooth motion. A set of $C_j \times C_k \times C_l \times C_t$ control points is placed uniformly in space and time. Each control point is assigned a displacement vector, forming the set of motion model parameters $\mathbb{S} = \{\boldsymbol{s}_{jklt} \in \mathbb{R}^3 \mid 1 \le j, k, l, t \le C_j, C_k, C_l, C_t\}$. Formally, the motion model is then given by

$$M(i, \boldsymbol{x}, \boldsymbol{s}) = \boldsymbol{x} + \sum_{j,k,l,t} B_j(x_0) B_k(x_1) B_l(x_2) B_t(i)\, \boldsymbol{s}_{jklt} \,, \tag{5}$$

where B_{j-t} are the cubic B-spline basis functions [14].

During the estimation of the motion model parameters, it needs to be ensured that only plausible motions are considered, i.e. no rapid motion or folding. This can be enforced by either a small number of control points or additional regularization [6], [10] during the optimization. In this paper the former approach is taken.

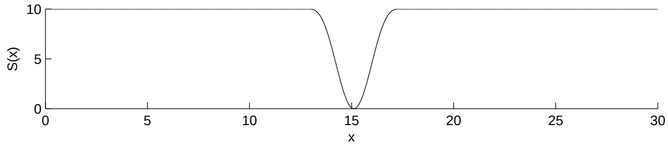

Fig. 2: Search space $S(x)$ for the parameters $a_s = 10, e_s = 3, c_t = 67, w_s = 20$. The number of projection images was set to $N = 133$ and the number of temporal control points to $C_t = 30$.

D. Motion Compensated FDK-Reconstruction

The formulation of our objective function for motion estimation (Sect. II-B) is based on a motion compensated reconstruction $f(\boldsymbol{x}, \boldsymbol{s})$. The function f returns the reconstructed object value at a voxel $\boldsymbol{x}$ based on the motion model parameters $\boldsymbol{s}$. In principle, any motion compensated reconstruction algorithm could be used. In this paper, an extension of the FDK reconstruction method for moving objects is utilized [4], [10]. It is given by

$$f(\boldsymbol{x}, \boldsymbol{s}) = \sum_i w(i, M(i, \boldsymbol{x}, \boldsymbol{s})) \cdot \hat{p}(i, A(i, M(i, \boldsymbol{x}, \boldsymbol{s}))) \,, \quad (6)$$

with $w : \{1, \ldots, N\} \times \mathbb{R}^3 \to \mathbb{R}$ being the distance weight in the FDK-formula and $\hat{p}$ being the preprocessed, filtered and redundancy weighted projection data.

E. Optimization Strategy

1) Constraining the Search Space: The search space during the optimization of (1) can be constrained due to the fact that we have a temporal focus of our reconstruction by the weighting function W_t. The closer a temporal control point is to the center c_t of the temporal weighting function, the smaller the expected motion is. If we further assume a maximum control point displacement a_s we can restrict the search space of a control point displacement to $\|\boldsymbol{s}_{jklt}\|_2 \le S(t)$

$$S(x) = a_s - \begin{cases} a_s \cos^{e_s}\left(\frac{\left|x\frac{N}{C_t} - c_t\right|}{w_s}\pi\right) & \text{if } \left|x\frac{N}{C_t} - c_t\right| \le \frac{w_s}{2} \\ 0 & \text{otherwise.} \end{cases} \quad (7)$$

In Fig. 2 an example of the search space S is depicted for $a_s = 10, e_s = 3, c_t = 67, w_s = 20$. The number of projection images was set to $N = 133$ and the number of temporal control points to $C_t = 30$.

2) Iteration Scheme: In general (1) can be optimized either using gradient-based methods or optimization procedures which do not require explicit knowledge of the gradient. The derivative of the objective function (3) with respect to the motion model parameters can be calculated analytically if the derivatives of the pixel-wise dissimilarity measure d and the motion compensated reconstruction function f can be calculated, too. This is the case e.g. for the squared error and the motion compensated FDK reconstruction.

However, in some cases the derivative may be noisy and the optimization can get easily trapped by local minima. In these situations optimization methods without the usage of gradients can be beneficial. We propose an iteration scheme which is based on the simultaneous perturbation stochastic approximation (SPSA) algorithm [15]. SPSA is especially efficient in high-dimensional problems in terms of providing a good solution for a relatively small number of measurements of the objective function. The essential feature of SPSA is the underlying gradient approximation that requires only two objective function measurements per iteration regardless of the dimension of the optimization problem.

(a) motion corrupted (b) motion corrected (c) no motion

Fig. 3: Volume rendering of the reconstructed phantom. The motion corrupted reconstruction ($\boldsymbol{s} = \boldsymbol{0}$) is depicted in (a). The motion compensated reconstruction is depicted (b). The ground truth reconstruction without motion is shown in (c). All images were obtained using the same visualization settings.

In each iteration the spatial control points which promise the best reduction of the objective function are selected for optimization using the SPSA algorithm. The optimization stops after I iterations. In detail, the the following iteration scheme is proposed for an efficient optimization of (1):

Step 1: Initialize $\boldsymbol{s}^0 = \boldsymbol{0}$.

Step 2: Dynamic backprojection of the temporally weighted pixel-wise dissimilarities:

$$g^n(\boldsymbol{x}, \boldsymbol{s}^n) = \sum_i W_t(i) d(p(i, \boldsymbol{u}), F(i, \boldsymbol{u}, \boldsymbol{s}^n)) \,,$$

with $\boldsymbol{u} = A(i, M(i, \boldsymbol{x}, \boldsymbol{s}^n))$.

Step 3: Resampling of the dynamic backprojection onto the $C_j \times C_k \times C_l$ spatial B-spline grid.

Step 4: Select the control point with the maximum error and J additional random control points. The likelihood of a point to be selected is proportional to its backprojection error. Thus it is more likely that points with high error values will be selected.

Step 5: Perform I_s iterations of the SPSA algorithm for the selected subset of control points.

Step 6: Set $n = n+1$. Stop if $n > I$, otherwise continue with step 2.

III. Numerical simulation

A. Methods

1) Phantom data: A synthetic cardiac vasculature phantom undergoing local deformations in combination with a global rigid motion has been used to generate motion corrupted projection data. The number of projection images was set to $N = 133$ covering an angular range of $200°$ in 5 seconds. The size of the projection images was set to 512×512 pixels. The heart rate of the phantom was set to 75 bpm leading to

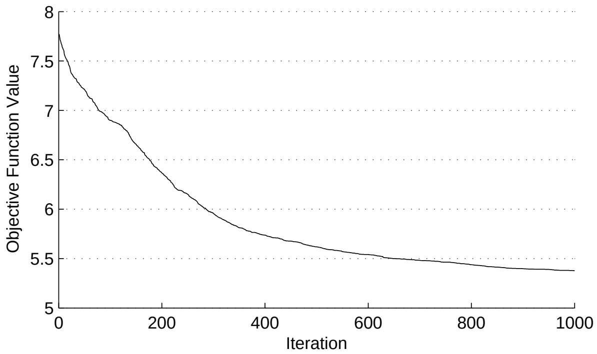

Fig. 4: Convergence behaviour of the iteration scheme for optimization without gradient calculation.

six observable heart beats in the projection data. A video of the moving phantom can be found online[1].

2) Parameter Selection for Motion Estimation: The size of the B-spline grid was set to $C_j = C_k = C_l = 5$ and $C_t = 30$. This sparse selection of B-spline control points guarantees a smooth motion. Thus, no additional regularizer has been used during optimization. As pixel-wise dissimilarity measure the squared error $d(x, y) = (x-y)^2$ has been used. The parameters of the optimization were set to $I = 1000, I_s = 30, J = 4$. The parameters for the temporal weighting function and search space were set to $e_t = 1.5, c_t = 67, w_t = 133$ and $a_s = 15$ mm$, e_s = 3, w_s = 20$, respectively. The size of the reconstructed volume was set to 128^3 voxels with an isotropic voxel size of 1 mm.

B. Results

In figure 3b the motion compensated reconstruction using the estimated motion parameters is depicted. It can be seen that the motion could be recovered well and that the motion compensated reconstruction is of comparable quality to the non-moving ground truth phantom reconstruction. The convergence behaviour of the algorithm is depicted in figure 4. The runtime for the presented setup was in average 5 minutes per iteration on the NVIDIA Quadro FX5600 graphics card using a CUDA 2.0 implementation.

IV. Conclusion and Outlook

Motion estimation is one of the most demanding issues to be addressed in the cardiac reconstruction literature. In this paper a framework for estimating motion was presented. Motion estimation is formulated as optimization problem requiring solely the estimation of motion model parameters. This could be achieved by exploiting the availability of motion compensated reconstruction algorithms. Those algorithms provide a high quality reconstruction of a moving object assuming the motion is known. Compared to methods estimating the object function and the motion our method decreases significantly the number of unknowns. In a numerical simulation study it could be shown that the method is capable of recovering deformable motion without prior assumptions about the periodicity of the motion.

In summary a promising framework laying out the foundation for many future applications was presented. Our future research will focus on accelerating the runtime and testing on clinical data.

Disclaimer: The concepts and information presented in this paper are based on research and are not commercially available.

[1] http://www5.informatik.uni-erlangen.de/en/our-team/rohkohl-christopher/projects/motion-compensated-cardiac-reconstruction-using-c-arm-ct/

References

[1] N. Strobel, O. Meissner, J. Boese, T. Brunner, B. Heigl, M. Hoheisel, G. Lauritsch, M. Nagel, M. Pfister, E.-P. Rhrnschopf, B. Scholz, B. Schreiber, M. Spahn, M. Zellerhoff, and K. Klingenbeck-Regn, *Multislice CT*, 3rd ed. Springer Berlin Heidelberg, 2009, ch. 3D Imaging with Flat-Detector C-Arm Systems, pp. 33–51.

[2] B. Desjardins and E. Kazerononi, "ECG-Gated Cardiac CT," *American Journal of Roentgenology*, vol. 182, no. 4, pp. 993–1010, April 2004.

[3] G. Lauritsch, J. Boese, L. Wigstrm, H. Kemeth, and R. Fahrig, "Towards cardiac c-arm computed tomography." *IEEE Transactions on Medical Imaging*, vol. 25, no. 7, pp. 922–934, July 2006.

[4] D. Schäfer, J. Borgert, V. Rasche, and M. Grass, "Motion-compensated and gated cone beam filtered back-projection for 3-d rotational x-ray angiography." *IEEE Transactions on Medical Imaging*, vol. 25, no. 7, pp. 898–906, July 2006.

[5] E. Hansis, D. Schafer, O. Dossel, and M. Grass, "Evaluation of iterative sparse object reconstruction from few projections for 3-d rotational coronary angiography," *IEEE Transactions on Medical Imaging*, vol. 27, no. 11, pp. 1548–1555, November 2008.

[6] C. Blondel, G. Malandain, R. Vaillant, and N. Ayache, "Reconstruction of coronary arteries from a single rotational x-ray projection sequence," *IEEE Transactions on Medical Imaging*, vol. 25, no. 5, pp. 653–663, May 2006.

[7] L. Desbat, S. Roux, and P. Grangeat, "Compensation of some time dependent deformations in tomography," *IEEE Transactions on Medical Imaging*, vol. 26, no. 2, pp. 261–269, February 2007.

[8] K. Taguchi and H. Kudo, "Motion compensated fan-beam reconstruction for computed tomography using derivative backprojection filtering approach," in *9th Int. Meeting on Fully 3D Image Reconstruction in Radiology and Nuclear Medicine*, Lindau, Germany, July 2007, pp. 433–436.

[9] M. Prümmer, L. Wigstroem, J. Hornegger, J. Boese, G. Lauritsch, N. Strobel, and R. Fahrig, " Cardiac C-arm CT: Efficient Motion Correction for 4D-FBP ," in *Nuclear Science Symposium, Medical Imaging* , October 2006.

[10] C. Rohkohl, G. Lauritsch, A. Nöttling, M. Prümmer, and J. Hornegger, "C-arm ct: Reconstruction of dynamic high contrast objects applied to the coronary sinus," in *IEEE NSS-MIC (Nuclear Science Symposium-Medical Imaging Conference)*, Dresden, Germany, October 2008, pp. M10–328.

[11] H. Schomberg, "Time-resolved cardiac cone beam ct," in *9th Int. Meeting on Fully 3D Image Reconstruction in Radiology and Nuclear Medicine*, Lindau, Germany, July 2007, pp. 362–365.

[12] E. Hansis, H. Schomberg, K. Erhard, O. Dössel, and M. Grass, "Four-dimensional cardiac reconstruction from rotational x-ray sequences: first results for 4d coronary angiography," E. Samei and J. Hsieh, Eds., vol. 7258, no. 1. Lake Buena Vista, FL, USA: SPIE, March 2009, p. 72580B.

[13] E. Hansis, D. Schäfer, O. Dössel, and M. Grass, "Projection-based motion compensation for gated coronary artery reconstruction from rotational x-ray angiograms," *Physics in Medicine and Biology*, vol. 53, no. 14, pp. 3807–3820, July 2008.

[14] M. Unser, "Splines: A perfect fit for signal and image processing," *IEEE Signal Processing Magazine*, vol. 16, no. 6, pp. 22–38, November 1999, IEEE Signal Processing Society's 2000 magazine award.

[15] J. C. Spall, "Overview of the simultaneous perturbation method for efficient optimization," *Johns Hopkins APL Technical Digest*, vol. 19, no. 4, pp. 482–492, October 1998.